Available online at www.sciencedirect.com

ScienceDirect

IFAC Papers Online CONFERENCE PAPER ARCHIVE

IFAC PapersOnLine 50-1 (2017) 4400–4405

Spatially Continuous Modeling and Control of Swing Dynamics in Electric Power Grids ⋆

Lea Sirota and **Anuradha M. Annaswamy**

Department of Mechanical Engineering, Massachusetts Institute of Technology, Cambridge, MA 02139, USA.
E-mail: {lbeilkin,aanna}@mit.edu.

Abstract: We propose a new control approach for swing oscillation suppression in large power grids, based on a spatially continuous representation of the system. Traditional modeling is spatially discrete irrespective of the grid size, perceiving the swing dynamics as frequency and phase oscillations. However, we show that for long chains of generators the overall swing dynamics is essentially governed by propagating electro-mechanical waves, retrieving the oscillations only locally. We therefore model the system by partial differential equations, where we decompose the grid into open and closed ended chains of generators, strings and rings. The key principle of the proposed approach is generation of uni-directional control waves that achieve closed loop matching of measured disturbance waves. While in strings this is naturally implemented by actuation at the boundary, the lack of boundaries in rings poses significant challenges. We solve the problem by introducing a new method for interior generation of near exact uni-directional waves. The method, which we denote by Interior Wave Suppression control, requires a minimal number of concentrated actuation and measurement devices for a given ring.

Keywords: Power systems, swing oscillation, electro-mechanical waves, wave suppression.

1. INTRODUCTION

Control of swing dynamics is a ubiquitous element of a large power network, where widely dispersed generators are interconnected through tielines. The essential characteristic that provides flawless power transmission through the network is synchronized rotation of all generators. However, in the presence of any disturbances, which may be caused due to various reasons including generation trips and outages or load changes, asynchronous motion can result. Such a motion leads to oscillations in the rotation frequency and angle, which poses a serious concern, as it can lead to increasing frequency swings and therefore brown-outs and black-outs. This problem has been addressed extensively and is the subject of numerous publications, e.g. Chakrabortty (2012); Mhaskar and Kulkarni (2006); Deng and Zhang (2014). Most of the existing approaches are based on spatially discrete modeling, implemented by ordinary differential equations (ODEs), and focus on analysis and synthesis using the ODE-models.

Our thesis, in contrast, is that for large power grids the fundamental mechanism that produces the phase and frequency oscillations is a continuous one. We argue that the swing dynamics in a string of power generators is the electrical analogue of vibrations in a mechanical string, with the generators as the inertia and the tieline admittance as the string tension. Transmitting power over the grid is therefore equivalent to sending a wave through the string. As we demonstrate in the sequel by simulating the discrete model, as the number of generators on a line becomes larger, the overall swing dynamics evolves into traveling electro-mechanical waves, preserving the oscillations as a local effect only. The existense and propagation of electro-mechanical waves through the grid was also independently recorded by extensive simulations in Tsai et al. (2007). This characteristic suggests modeling the system by partial differential equations (PDEs) rather than ordinary ones. As a result, accurate and physically oriented methods for mitigating and suppressing the disturbance waves are better realized through the use of PDEs.

Indeed, the problem of modeling and controlling the swing dynamics as a continuum has been examined in several research studies. In Cresap and Hauer (1981), the swing of a string of generators was modeled by an undamped wave equation. PDE modeling of more complex grid configurations including two-dimensional topology and various losses was carried out in Thorp et al. (1998) and Parashar et al. (2004), where inclusion of wind penetration was considered in Gayme and Chakrabortty (2012). In Magar et al. (2014), adaptive control of a continuously modeled string grid was designed using finite eigenmode discretization of the PDE. In Sahyoun et al. (2015), optimal control algorithm was designed for the exact one dimensional PDE. In Lesieutre et al. (2002), boundary controllers were designed for one and two dimensional lossless grids, which eliminated wave reflection from the boundaries.

The approach we present in this paper is different first all due to regarding a general two dimensional grid topology as a collection of interconnected open and closed ended one dimensional chains of generators, denoted by strings and rings, respectively. Assuming that a large number of generators is spanned along each chain, we model the chains by one dimensional wave equations, distinguishing strings from rings by appropriate end conditions. For each of these two building blocks of the grid we employ infinite dimensional transfer functions to design an accurate, physically oriented control method, which fully utilizes the exact PDE-structure by exploiting the system traveling wave characteristics.

The key element of the proposed method is a special mech-

⋆ This work was supported in part by the MIT-Technion Program and in part by the National Science Foundation grants ECCS- 1135815 and EFRI-1441301.

10.1016/j.ifacol.2017.08.891

anism that generates near uni-directional control waves that are designed to match the disturbance waves via closed loop algorithms. The uni-directional characteristic is crucial for the controllers not to create themselves back action disturbance waves. For strings this is implemented as boundary control, i.e. by a concentrated actuation at a string end, which naturally generates a wave traveling only at a single direction. The control working principle can then be considered as an absolute absorption of waves incoming into the actuated end, thus preventing their further reflections (which can be also regarded as mechanical impedance matching). The approach then coincides with the previously reported Absolute Vibration Suppression (AVS) method, originally designed in Halevi (2005) to control one-dimensional mechanical flexible structures governed by the undamped wave equation. It was further extended in Sirota and Halevi (2015b) and Sirota and Halevi (2015a) to more general forms of it, accounting for in-domain damping and elasticity. The approach in Lesieutre et al. (2002), though differently derived, is essentially equivalent.

For rings, however, any concentrated actuation is inherently interior, which means it generates two waves traveling in opposite directions. Blocking wave propagation by concentrated interior actuation therefore becomes a highly nontrivial task. Our solution includes designing a special combination of a small number of concentrated actuators and sensors to produce a control wave, which approaches to be uni-directional to the extent that control effort is available. Incorporation of modern power systems control devices, such as the Thyristor Controlled Series Compensator (TCSC), which is a Flexible AC Transmission Systems (FACTS) device and Phasor Measurement Units (PMU), Chakrabortty (2012)-Chakrabortty and Khargonekar (2013), makes the proposed control method readily implementable. We denote the method by Interior Wave Suppression.

2. EXACT TRAVELING WAVE MODEL

In Sec. 2.1 we derive traveling wave models for swing dynamics of string and ring elements, which are illustrated in Fig. 1. In Sec. 2.2 we represent the PDE associated with the spatially continuous system through infinite dimension transfer functions (TFs), which capture the propagating wave nature of swing oscillations in the grid.

2.1 The Continuous Model in Time Domain

The commonly used model for swing dynamics of the i_{th} generator interconnected with K other (identical) generators is spatially discrete, and is given, e.g. in Anderson and Fouad (2008), by

$$\frac{2HS}{\Omega}\ddot{\delta}_i + B\dot{\delta}_i = P_i^M - \sum_{k=1,k\neq i}^{K} \frac{E_i E_k}{X_{i,k}} \sin(\delta_i - \delta_k). \qquad (1)$$

The variables $\delta_i(t)_{[r]}$ and $\dot{\delta}_i(t)_{[r/s]} = \omega_i(t) - \Omega$ are relative swing angle and frequency, respectively, of the i_{th} generator, $\Omega = 60_{[Hz]}$ is the base frequency, $H_{[s]}$ is the inertia constant, $S_{[MW]}$ is the generation rating, $P^M_{i[MW]}$ is the mechanical power. The normalized voltage $E_{i[p.u.]}$ equals 1 and the normalized reactance of the line segment i,k is constant, $X_{i,k[MW^{-1}]} = X$, due to the even spacing assumed. The damping B represents system losses augmented with secondary control, which keeps zero steady state swing frequency error, Sauer and Pai (1998).

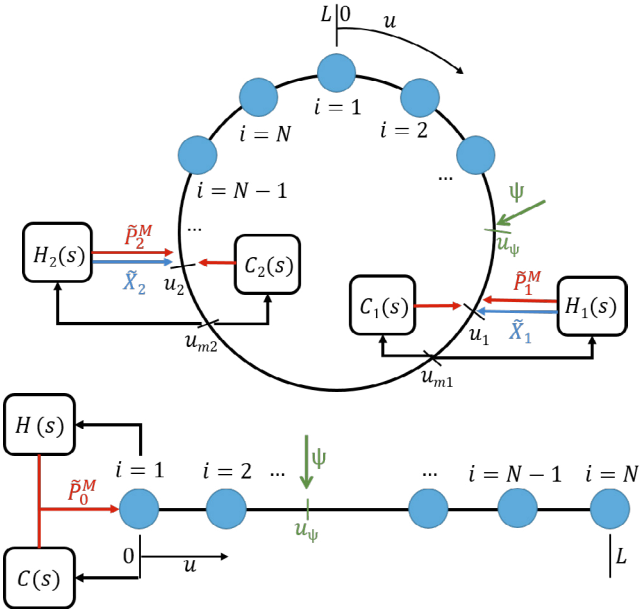

Fig. 1. Basic elements of power grid topology comprising N generators evenly interconnected through tie-lines of total length L. Top: closed-ended element - a ring. Bottom: open-ended element - a string. ψ is a power disturbance. The Wave Suppression control setup with controllers $H(s)$, $C(s)$ and control signals $\tilde{P}^M$, $\tilde{X}$ is designed in Sec. 3.

Since in strings and rings each generator is connected only to its direct previous and forthcoming neighbors, the model (1), for small angle deviations, takes the form

$$\frac{2HS}{\Omega}\ddot{\delta}_i + B\dot{\delta}_i = P_i^M - \frac{1}{X}(\delta_{i+1} - 2\delta_i + \delta_{i-1}). \qquad (2)$$

For (2) to evolve into a spatially continuous system, the distance between two adjacent generators, L/N, should be viewed as an infinitesimal perturbation ε in the spatial coordinate. That is, setting locations i and $i+i$ in (2) as u and $u+\varepsilon$, we can rewrite (2) as

$$\frac{2H}{\Omega}\frac{S}{\varepsilon}\ddot{\delta}(u,t) + \frac{B}{\varepsilon}\dot{\delta}(u,t) = \frac{1}{\frac{X}{\varepsilon}}\frac{\delta(u+\varepsilon,t) - 2\delta(u,t) + \delta(u-\varepsilon,t)}{\varepsilon^2}. \qquad (3)$$

Letting $\varepsilon \to 0$, with the subscripts u and t denoting partial derivatives, (3) becomes

$$\frac{2Hs}{\Omega}\delta_{tt}(u,t) + b\delta_t(u,t) = p^M(u,t) - \frac{1}{x}\delta_{uu}(u,t), \qquad (4)$$

where $s = \frac{1}{\varepsilon}S$, $x = \frac{1}{\varepsilon}X$, $b = \frac{1}{\varepsilon}B$ and p^M is a spatially distributed deviation in mechanical power. Equation (4) is the well-known damped wave equation, Graff (1975), and it coincides with the continuous model of the swing dynamics originally derived in Cresap and Hauer (1981). Bringing (4) to a canonical form and designating p^M as a power disturbance per unit length, ψ, we obtain

$$c^2\delta_{uu}(u,t) = \delta_{tt}(u,t) + \beta\delta_t(u,t) + \tfrac{1}{\rho}\psi(u,t), \qquad (5)$$

where $\beta = b/\rho$ and c is the electro-mechanical wave propagation speed, given in terms of the equivalent string tension T and linear density ρ, by

$$c = \left(\frac{T}{\rho}\right)^{1/2}, \qquad T = \frac{1}{x}, \qquad \rho = \frac{2Hs}{\Omega}. \qquad (6)$$

While the equivalent continuous system of (2) in the form of (4) requires that ε be arbitrarily small, numerical simulations shown in the example in Sec. 2.2 illustrate that the solutions of the two systems, for typical values suggested in Cresap and Hauer (1981), coincide even for $\varepsilon \sim 20$ miles.

The related end conditions depend on which topology in Fig. 1 is being considered. In a string there should be no power flow through the ends, i.e. free (Newmann) boundary conditions, whereas in a ring we require position and power continuity, leading to

$$\begin{aligned} &\delta_u(0,t) = \delta_u(L,t) = 0; && \textit{string}, \\ &\delta(0,t) = \delta(L,t), \quad \delta_u(0,t) = \delta_u(L,t); && \textit{ring}. \end{aligned} \tag{7}$$

2.2 Transfer Function Representation

The intrinsic way of obtaining the exact traveling wave behavior of the system that is ready for a wave oriented control is via representing the PDE (5) by its corresponding infinite dimensional TF in the complex domain s. The TF of the damped wave equation was derived in Sirota and Halevi (2015a), where it was shown to be of fractional order in s, leading to nontrivial time domain interpretation. Since our goal here is to deliver the main idea of wave propagation in swing dynamics, we present the TF derivation and the analysis thereafter for the simplified undamped case, $\beta = 0$. However, the damping is assumed to exist throughout the sequel, which is essential in the control section 3. Applying Laplace transform to (5) with respect to time, yields

$$\delta_{uu}(x;s) = \left(\tfrac{s}{c}\right)^2 \delta(u;s) - \tfrac{1}{T}\psi(u;s). \tag{8}$$

The total solution of (8), which is a second order ODE in u, with s as a parameter, is given by

$$\delta(u;s) = \int_0^L G(u,\xi;s)\psi(\xi;s)\mathrm{d}\xi, \tag{9}$$

where $G(u,u_\psi;s)$ is the TF from a spatially concentrated disturbance $\Psi(s)$ acting at u_ψ to the swing angle deviation $\delta(u;s)$. For a string the TF becomes

$$\begin{aligned} G_s(u;s) = &\frac{e^{-|\tau_u-\tau_\psi|s} + R_L e^{-(2\tau-|\tau_u-\tau_\psi|)s}}{2\phi s\Delta_s(s)} \\ &+ \frac{R_0 e^{-(\tau_u+\tau_\psi)s} + R_0R_L e^{-(2\tau-\tau_u-\tau_\psi)s}}{2\phi s\Delta_s(s)} \end{aligned} \tag{10}$$

and for a ring

$$G_r(u;s) = \frac{e^{-|\tau_u-\tau_\psi|s}}{2\phi s\Delta_r(s)} + \frac{e^{-(\tau-|\tau_u-\tau_\psi|)s}}{2\phi s\Delta_r(s)}, \tag{11}$$

where

$$\Delta_s(s) = 1 - R_0R_L e^{-2\tau s}, \qquad \Delta_r(s) = 1 - e^{-\tau s}, \tag{12}$$

and

$$\tau = \frac{L}{c}, \quad \tau_u = \frac{u}{c}, \quad \tau_\psi = \frac{u_\psi}{c}, \quad \phi = \frac{T}{c}, \quad R_{0,L} = 1. \tag{13}$$

Being infinite dimensional, (10) and (11) describe the simultaneous action of all system modes, thus implying traveling waves. In particular, the response to the spatially concentrated disturbance causes two waves to be generated, including progressive and regressive components, which respectively move to the right vs. left in a string, and clockwise vs. counterclockwise in a ring. These two waves are captured by the first and the second terms of each TF, respectively.

Each wave propagates along the structure with speed c and completes a full cycle, i.e. returns to its origin, after 2τ time units in a string and τ in a ring. The difference is due to the reflection process that occurs in the string. The first cycle of motion is represented by the TFs numerator, where the time constants at the exponents indicate the appropriate wave arrival times from u_ψ to u. The proceeding cycles are represented by the infinite series expansion

$$\frac{1}{\Delta_s(s)} = \sum_{k=0}^{\infty} (R_0R_L)^k e^{-2k\tau s}, \quad \frac{1}{\Delta_r(s)} = \sum_{k=0}^{\infty} e^{-k\tau s}. \tag{14}$$

The reflection effect depends on the nature of the boundary condition, and is quantified by the exponent amplitudes R_0 and R_L, denoted by reflection coefficients. In the current case of free ends we have $R_0 = R_L = 1$, hence a wave that hits a free boundary is reflected identically. The wave shape during motion is determined by the exponent powers. While angular position is the shifted input integration due to the rigid body mode, angular velocity is simply a shift of the input. A detailed discussion of the propagation and reflection process in strings can be found in Halevi (2005) and Sirota and Halevi (2013). The traveling wave nature of the power grid is illustrated in the following example.

Example 2.1. Consider a string of total length of $L = 6400_{[km]}$ with $N = 200$ generators. Each generator is characterized by $H = 5_{[s]}$ and $S = 375_{[MW]}$, whereas the total line reactance is given by $X_{tot} = 0.0031_{[MW^{-1}]}$. The equivalent continuous system parameters are then given by $c = 2560_{[km/s]}$, $\tau = 2.5_{[s]}$ and $\phi = 797_{[MW\cdot s/km]}$.

The response of the swing frequency by the discrete dynamics as given in (2) and that of the corresponding continuous system (5), at $u = \frac{1}{4}L$ for a concentrated pulse disturbance ψ at $u_\psi = \frac{1}{2}L$, were simulated and shown in Fig. 2 (in the form of blue and black lines, respectively). The two graphs completely coincide, which clearly demonstrates that the underlying swing dynamics can be represented effectively by a spatially continuous system. Fig. 3 illustrates how a disturbance that begins at the center of the string generates two electro-mechanical waves that propagate to the left and right and get reflected at the boundaries, exactly as predicted by the TF (10). This confirms that the oscillations observed in Fig. 2 are only a local effect of the overall wave phenomenon.

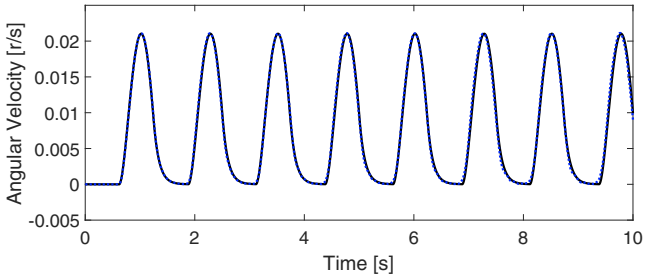

Fig. 2. Swing Frequency at $u = \frac{1}{4}L$ of the string in Example 2.1 for $u_\psi = \frac{1}{2}L$. Black - continuous model (5). Blue - discrete model (2).

3. WAVE SUPPRESSION CONTROL ALGORITHM

In this section we design a closed loop control method that attenuates oscillations in the swing frequency $\dot{\delta}(u,t)$ by suppressing the propagation of the electro-mechanical disturbance wave, captured by the continuous model (5). In particular, the

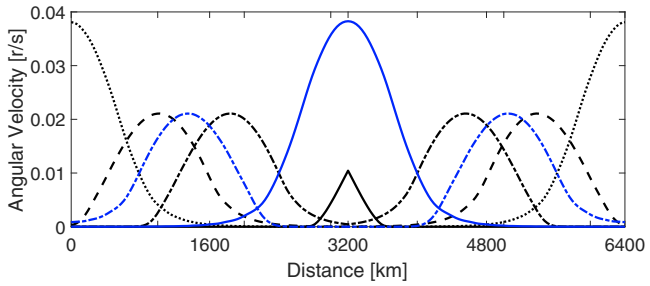

Fig. 3. Swing Frequency of the string in Example 2.1 for $u_\psi = \frac{1}{2}L$. The response is plotted at different time instances $0 < t_1 < t_2 < t_3 < t_4 < t_5 < t_6 < \tau$ for the entire string. Black - the initial wave before reflection from the boundaries: t_1 (solid), t_2 (dashed-dotted), t_3 (dashed), t_4 (dotted). Blue - the wave after first reflection: t_5 (dashed-dotted), t_6 (solid).

control action includes generating a wave as similar as possible to the disturbance wave with the opposite sign, and scheduling its injection to the grid to match the disturbance, thus creating a net zero motion. The actual control mechanism in the string case coincides with the AVS method introduced in Sec. 1, and its application to the string power grid element is given in Sec. 3.1. The actuation is carried out by mechanical power delivery (a concentrated force in a mechanical string analogy) to an end generator, denoted by $\widetilde{P}_0^M$ in Fig. 1-bottom. For a collocated setup we place the sensor and actuator at the left end ($u = 0$ in the scheme), and design the controller $H(s)$ (and possibly $C(s)$).

In a ring topology, however, the lack of boundaries implies that a single concentrated input acting at any location will generate two waves (see the discussion in Sec. 2.2). In Sec. 3.2 we suggest the Interior Wave Suppression methodology of generating in-domain near exact uni-directional waves, or equivalently, creating artificial interior boundaries. The main idea is affecting the spatial derivative of the system. Ideally, this could be achieved by application of a pair of opposite concentrated inputs at zero distance between each other. However, this is physically impossible, as it will result in a non causal actuation system. The practical implication is therefore the trade-off between exactness of wave direction and control effort. We employ two concentrated control pairs, where one is responsible for elimination of the progressive disturbance wave and the other of the regressive. Each pair is applied at two adjacent points, u_1, $u_1+\varepsilon$ and u_2, $u_2+\varepsilon$ in Fig. 1-top, i.e. a total of only four actuators. The control action can be carried out either by mechanical power $\widetilde{P}^M$ at all the four points. An alternative way, which is adopted in this work, is combining $\widetilde{P}^M$ at u_1 and u_2 with a different kind of actuation, namely a change of reactance $\widetilde{X}_j$ beyond the nominal value X of the corresponding line segments between u_j and $u_j+\varepsilon$, $j = 1,2$. $\widetilde{X}$ may be implemented by the emerging TCSC devices (Sec. 1), analogous to local change of tension in a mechanical string. We place two corresponding sensors at locations u_{m_1} and u_{m_2}, which are not assumed collocated but satisfy $u_1 < u_{m_1} < u_{m_2} < u_2$, and design the controllers $H_j(s)$ and $C_j(s)$.

3.1 Boundary Wave Suppression (or AVS) Control of the String

The control action by $\widetilde{P}_0^M$ at the leftmost generator (Fig. 1-top) is expressed in the continuous model (5) through the boundary condition

$$\delta_u(0,t) = -\tfrac{1}{T}\widetilde{P}_0^M(t). \tag{15}$$

Since the controlled variable is the swing frequency $\dot{\delta}(u,t)$, the measured signal at $u = 0$ is $\dot{\delta}(0,t)$, denoted by $v(0;s)$ after Laplace transformation. The control signal is thus given by

$$\widetilde{P}_0^M(s) = -H(s)v(0;s), \tag{16}$$

where the expression for $v(0;s) = s\delta(0;s)$ is obtained from (10). To achieve the Wave Suppression goal (i.e. generating the opposite disturbance matching control wave), as a boundary controller, $H(s)$ should eliminate the wave reflections from that boundary, i.e. to completely absorb the waves incoming at $u = 0$. The mathematical implication is canceling out the exponent of the characteristic equation $\Delta_s(s)$ in (12), retaining only the first cycle of wave propagation. In the nominal undamped system (10) the controller is given by

$$H(s) = \phi, \tag{17}$$

where the constant ϕ, defined in (13), is the characteristic mechanical impedance of the string. The resulting constant rate feedback (16) is actually an active boundary damper. The closed loop TF from the disturbance $\Psi(t)$ to the swing frequency at any location $0 \le u \le L$, becomes

$$\frac{v_{CL}(u;s)}{\Psi(s)} = \frac{1}{2\phi}\left(e^{-|\tau_u-\tau_{u_0}|s} + e^{-(2\tau-|\tau_u-\tau_{u_0}|)s}\right), \tag{18}$$

which coincides with (10) for an effective reflection coefficient of $R_0 = 0$, indeed indicating a complete wave absorption.

We analyze the closed loop system stability via the input-output stability criterion, requiring that TFs from all possible exogenous signals to all outputs are stable. We carry out the proof by a straightforward calculation (suppressed here for brevity), yielding that all the TFs in the loop are given by a finite summation of delay exponents, similarly to (18), and thus are obviously stable. For the realistic damped system, where the exponents are of fractional order in s (i.e. no longer pure delays), stability proof of each TF is more involved and is given in detail in Sirota and Halevi (2015a). Control of the swing angle $\delta(u,t)$ is usually not required in the context of swing oscillation suppression. However, after closing the $\dot{\delta}(u,t)$ loop with (17), control of $\delta(u,t)$ reduces to the well-explored problem of control of rational systems (here an integrator) with delays via dead time compensators (DTC), Smith (1957). The additional controller $C(s)$ should then be used.

The resulting closed loop behavior of $\dot{\delta}(u,t)$ in Example 2.1 is illustrated in Fig. 4. As expected, the response contains only the first cycle of motion (out of infinitely many open loop cycles shown in Fig. 2). The coinciding responses of the discrete and continuous models (2) and (5) pinpoint that traveling wave behavior is intrinsic to large power grids.

3.2 Interior Wave Suppression Control of the Ring

We begin from incorporating the mechanical power and reactance actuators pairs in the discrete model (2) and derive the corresponding TFs for the continuous model (5). In the linear swing equation (2) for generators i and $i+1$, linearized about an electrical power flow $\overline{P}^E_{i,i+1} \doteq \overline{P}^E$, the reactance actuators $\widetilde{X}_{i,i+1} \doteq \widetilde{X}_j$ appear as a pair of power inputs at adjacent points u_i and u_{i+1} that correspond to locations u_j and $u_j+\varepsilon$, $j = 1,2$, in Fig. 1 for certain choices of i. Together with the counterpart mechanical power $\widetilde{P}_j^M$ input at u_j, we obtain

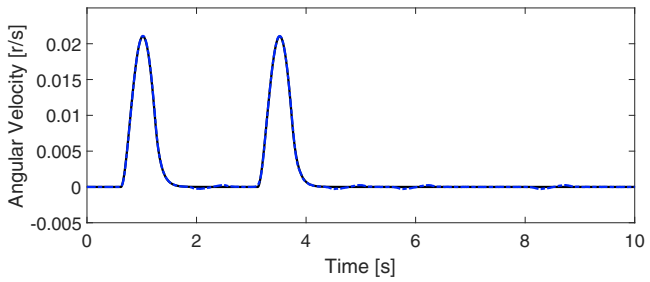

Fig. 4. Swing frequency at $u=\frac{1}{4}L$ in closed loop with controller (17) of the string system in Example 2.1 for $u_\psi=\frac{1}{2}L$. Only first cycle of motion exists. Black - continuous model (5). Blue - discrete model (1).

$$\begin{aligned}\frac{2HS}{\Omega}\ddot{\delta}_i &= \frac{1}{X}\left[\delta_{i+1}-2\delta_i+\delta_{i-1}\right]+\frac{\overline{P}^E}{X}\widetilde{X}_j+\widetilde{P}_j^M,\\ \frac{2HS}{\Omega}\ddot{\delta}_{i+1} &= \frac{1}{X}\left[\delta_{i+2}-2\delta_{i+1}+\delta_i\right]-\frac{\overline{P}^E}{X}\widetilde{X}_j.\end{aligned} \tag{19}$$

By (11), the TF from $\widetilde{P}_j^M$ and $\widetilde{X}_j$ to the swing frequency then becomes

$$v(u;s)=\frac{1}{2\phi\Delta_r(s)}\left(E_{P_j}(u;s)\widetilde{P}_j^M(s)+\frac{\overline{P}^E}{X}E_{X_j}(u;s)\widetilde{X}_j(s)\right) \tag{20}$$

where

$$E_{P_j}(u;s)=e^{-|\tau_u-\tau_{u_j}|s}+e^{-\left(\tau-|\tau_u-\tau_{u_j}|\right)s} \tag{21a}$$

$$E_{X_j}(u;s)=e^{-|\tau_u-(\tau_{u_j}+\tau_\varepsilon)|s}+e^{-(\tau-|\tau_u-(\tau_{u_j}+\tau_\varepsilon)|)s}-E_{P_j}(u;s), \tag{21b}$$

where following (13), $\tau_{u_j}=\frac{u_j}{c}$ and $\tau_\varepsilon=\frac{\varepsilon}{c}$. We begin by designing the $H_j(s)$ loops and set the control laws to be

$$\begin{aligned}\widetilde{P}_1^M &= -H_1(s)v_F^-(u_{m_1};s), & \widetilde{P}_2^M &= -H_2(s)v_F^+(u_{m_2};s),\\ \widetilde{X}_1 &= \frac{1}{\overline{P}^E\phi}H_1(s)\delta_F^-(u_{m_1};s), & \widetilde{X}_2 &= -\frac{1}{\overline{P}^E\phi}H_2(s)\delta_F^+(u_{m_2};s),\end{aligned} \tag{22}$$

where

$$H_1(s)=H_2(s)=\phi \tag{23}$$

coincides with (17). We now explain the feedback signals in (22), which are the filtered (F) regressive ($-$) swing frequency (v) and phase (δ) waves at u_{m1} and their progressive counterparts ($+$) at u_{m2}. The isolation of a directional wave out of a total measurement is a matter of programming. For ease of derivation we use the obvious relation $\delta(u;s)=\frac{1}{s}v(u;s)$, which leads to the equivalent form of the reactance laws $\widetilde{X}_1=\frac{1}{\overline{P}^E\phi s}\widetilde{P}_1^M$ and $\widetilde{X}_2=-\frac{1}{\overline{P}^E\phi s}\widetilde{P}_2^M$, and

$$\begin{aligned}v^-(u_{m_1};s) &= \frac{1}{2\phi\Delta_r(s)}\left(E_\psi^-(u_{m1};s)\Psi+\sum_{j=1}^{2}E_j^-(u_{mj};s)\widetilde{P}_j^M\right),\\ v^+(u_{m_2};s) &= \frac{1}{2\phi\Delta_r(s)}\left(E_\psi^+(u_{m2};s)\Psi+\sum_{j=1}^{2}E_j^+(u_{mj};s)\widetilde{P}_j^M\right).\end{aligned} \tag{24}$$

The terms $E_\psi^-(u_{m1};s)$ and $E_\psi^+(u_{m2};s)$ depend on the location of Ψ, for example for $u_{m1}<u_\psi<u_{m2}$, $E_\psi^-(u_{m1};s)=e^{-(u_\psi-u_{m1})s}$ and $E_\psi^+(u_{m2};s)=e^{-(u_{m2}-u_\psi)s}$. Using (21) with $\frac{1}{X}=\frac{\phi c}{\varepsilon}$, gives

$$\begin{aligned}E_1^-(u_{m_1};s) &= e^{-(\tau-\tau_{m_1}+\tau_{u_1})s}\left(1-A^-(s)\right)\\ E_1^+(u_{m_2};s) &= e^{-(\tau_{m_2}-\tau_{u_1})s}\left(1-A^+(s)\right)\\ E_2^-(u_{m_1};s) &= e^{-(\tau_{u_2}-\tau_{m_1})s}\left(1+A^-(s)\right)\\ E_2^+(u_{m_2};s) &= e^{-(\tau-\tau_{u_2}+\tau_{m_2})s}\left(1+A^+(s)\right)\end{aligned} \tag{25}$$

where

$$A^-(s)=\frac{c}{\varepsilon s}\left(e^{-\tau_\varepsilon s}-1\right)\quad A^+(s)=\frac{c}{\varepsilon s}\left(e^{\tau_\varepsilon s}-1\right). \tag{26}$$

Letting $\varepsilon\to 0$, yields

$$\lim_{\varepsilon\to 0}\left\{A^-(s)\right\}=-1\quad\lim_{\varepsilon\to 0}\left\{A^+(s)\right\}=1, \tag{27}$$

and thus

$$\begin{aligned}&\lim_{\varepsilon\to 0}\left\{E_1^-(u_{m1};s)\right\}=2e^{-(\tau-\tau_{m_1}+\tau_{u_1})s},\quad\lim_{\varepsilon\to 0}\left\{E_1^+(u_{m2};s)\right\}=0,\\ &\lim_{\varepsilon\to 0}\left\{E_2^+(u_{m2};s)\right\}=2e^{-(\tau-\tau_{u_2}+\tau_{m_2})s},\quad\lim_{\varepsilon\to 0}\left\{E_2^-(u_{m1};s)\right\}=0.\end{aligned} \tag{28}$$

Therefore, as the distance between the generators decreases, $E_1^-(u_{m1};s)$ and $E_2^+(u_{m2};s)$ become regressive at u_{m1} and progressive at u_{m2} control waves, which are tuned by the laws (22) to match the correspondingly measured waves. However, since ε will never be equal to zero, there will be a remainder of a progressive control wave at u_{m1} and a regressive one at u_{m2}. Although the remainder is small, if it enters the feedback loop it will eventually lead to divergence. Since those are parts of the control signal, we are able to subtract them out of the measurement, namely feeding back the reduced signals

$$\begin{aligned}v_F^-(u_{m_1};s) &= \frac{1}{2\phi\Delta_r(s)}\left(E_\psi^-(u_{m1};s)\Psi+E_1^-(u_{m1};s)\widetilde{P}_1^M\right),\\ v_F^+(u_{m_2};s) &= \frac{1}{2\phi\Delta_r(s)}\left(E_\psi^+(u_{m2};s)\Psi+E_2^+(u_{m2};s)\widetilde{P}_2^M\right).\end{aligned} \tag{29}$$

Such reduction is appropriate due to our original assumption that damping exists, i.e. the roots of $\Delta_r(s)$ are stable. The total closed loop response still contains that remainder, but its amplitude will become smaller as ε decreases, and in any manner will eventually vanish due to damping.

However, since the the control laws for $\widetilde{X}_j$ effectively consist of integration of the $\widetilde{P}_j^M$ laws, the $H_j(s)$ loops are not sufficient to internally stabilize the system. This suggests invoking the additional $C_j(s)$ loops in Fig. 1, to control the swing angle $\delta(u;s)$, which contains the rigid body mode, the stable $H_j(s)$ loops closed system, and a delay. A reasonable choice of $C_j(s)$ is thus again a DTC, but due to the several actuation and measurement options, its design should be taken carefully. In this paper we employ only $C_1(s)$ for the DTC (and $C_2(s)=0$). The overall stability proof, which is not given here due to space limitations, is quite straightforward in the undamped case but more involved in the damped case, following similar lines as the proof in Sirota and Halevi (2015a).

Figure 5 demonstrates the swing frequency response of the system in Example 2.1 for a ring element under the action of the ring $H_j(s)$ controllers (22) and an appropriate $C_1(s)$ controller. The disturbance penetrates at $u_\psi=0.15L$, the actuation and measurement locations are respectively given by $u_1=0.35L$, $u_2=0.75L$, $u_{m_1}=0.45L$, $u_{m_2}=0.65L$. The open loop response (black) is plotted vs. the $H_j(s)$ loops only (blue) and vs. the total closed loop (red). The blue plot illustrates the process of wave motion termination in the ring. The red plot illustrates the response of the total loop. Figure 6 depicts the total loop control signals, which all converge to zero. Figure 7 shows the corresponding total closed loop angle response, which converges to zero at the entire ring.

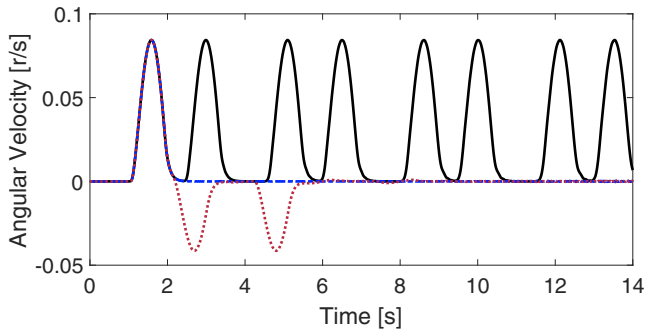

Fig. 5. Swing frequency at $u = \frac{1}{4}L$ for $u_\psi = 0.15L$ of the ring system in Example 2.1. Wave suppression demonstration. Black - open loop. Blue - closed loop with (22) only. Red - total closed loop.

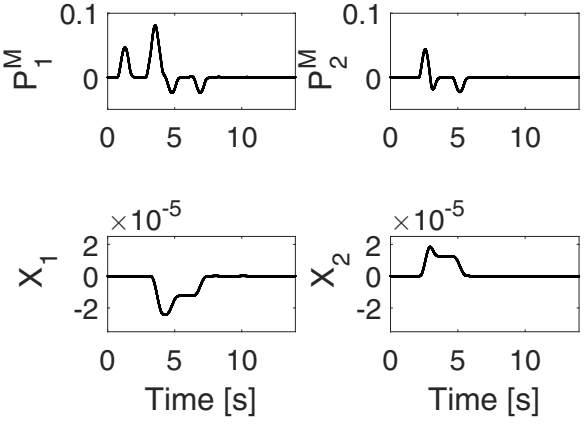

Fig. 6. Control signals of the total response in Fig. 5.

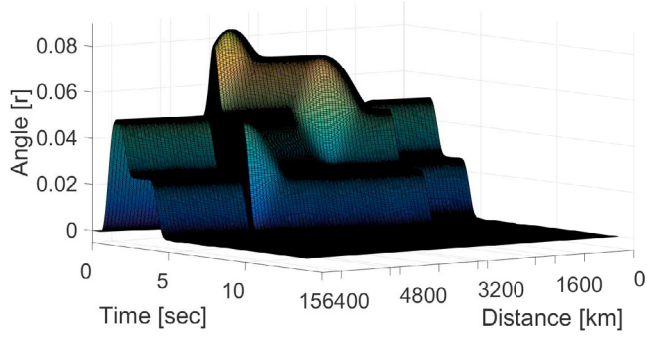

Fig. 7. Swing angle of the ring system in Example 2.1 for $u_\psi = 0.15L$. Total closed loop response is regulated to zero for all $0 \leq u \leq L$.

ACKNOWLEDGEMENTS

We would like to thank Dr. Aranya Chackrabortty for his insightful comments and suggestions.

REFERENCES

Anderson, P.M. and Fouad, A.A. (2008). *Power system control and stability*. John Wiley & Sons.

Chakrabortty, A. (2012). Wide-area damping control of power systems using dynamic clustering and TCSC-based redesigns. *Smart Grid, IEEE Transactions on*, 3(3), 1503–1514.

Chakrabortty, A. and Khargonekar, P.P. (2013). Introduction to wide-area control of power systems. In *American Control Conference (ACC), 2013*, 6758–6770. IEEE.

Cresap, R. and Hauer, J. (1981). Emergence of a new swing mode in the western power system. *IEEE Transactions on Power Apparatus and Systems*, 4(PAS-100), 2037–2045.

Deng, J. and Zhang, X.P. (2014). Robust damping control of power systems with TCSC: A multi-model bmi approach with H performance. *Power Systems, IEEE Transactions on*, 29(4), 1512–1521.

Gayme, D.F. and Chakrabortty, A. (2012). Impact of wind farm placement on inter-area oscillations in large power systems. In *American Control Conference (ACC), 2012*, 3038–3043. IEEE.

Graff, K.F. (1975). *Wave motion in elastic solids*. Courier Dover Publications.

Halevi, Y. (2005). Control of flexible structures governed by the wave equation using infinite dimensional transfer functions. *Journal of dynamic systems, measurement, and control*, 127(4), 579–588.

Lesieutre, B.C., Scholtz, E., and Verghese, G.C. (2002). Impedance matching controllers to extinguish electromechanical waves in power networks. In *Control Applications, 2002. Proceedings of the 2002 International Conference on*, volume 1, 25–30. IEEE.

Magar, K.T., Balas, M.J., and Gayme, D.F. (2014). Adaptive control of inter-area oscillations in wind-integrated power systems using distributed parameter control methods. In *American Control Conference (ACC), 2014*, 903–907. IEEE.

Mhaskar, U. and Kulkarni, A. (2006). Power oscillation damping using FACTS devices: modal controllability, observability in local signals, and location of transfer function zeros. *Power Systems, IEEE Transactions on*, 21(1), 285–294.

Parashar, M., Thorp, J.S., and Seyler, C.E. (2004). Continuum modeling of electromechanical dynamics in large-scale power systems. *Circuits and Systems I: Regular Papers, IEEE Transactions on*, 51(9), 1848–1858.

Sahyoun, S., Djouadi, S., Tomsovic, K., and Lenhart, S. (2015). Optimal distributed control for continuum power systems.

Sauer, P.W. and Pai, M. (1998). Power system dynamics and stability. *Urbana*.

Sirota, L. and Halevi, Y. (2013). Extended d'alembert solution of finite length second order flexible structures with damped boundaries. *Mechanical Systems and Signal Processing*, 39(1), 47–58.

Sirota, L. and Halevi, Y. (2015a). Fractional order control of flexible structures governed by the damped wave equation. In *American Control Conference (ACC), 2015*, 565–570. IEEE.

Sirota, L. and Halevi, Y. (2015b). Fractional order control of the two-dimensional wave equation. *Automatica*, 59, 152–163.

Smith, O.J. (1957). Closer control of loops with dead time. *Chemical Engineering Progress*, 53(5), 217–219.

Thorp, J.S., Seyler, C.E., and Phadke, A.G. (1998). Electromechanical wave propagation in large electric power systems. *Circuits and Systems I: Fundamental Theory and Applications, IEEE Transactions on*, 45(6), 614–622.

Tsai, S.J., Zhang, L., Phadke, A.G., Liu, Y., Ingram, M.R., Bell, S.C., Grant, I.S., Bradshaw, D.T., Lubkeman, D., and Tang, L. (2007). Frequency sensitivity and electromechanical propagation simulation study in large power systems. *Circuits and Systems I: Regular Papers, IEEE Transactions on*, 54(8), 1819–1828.